Marine plastics alter the organic matter composition of the air-sea boundary layer, with influences on CO_2 exchange: a large-scale analysis method to explore future ocean scenarios

List of authors:

Luisa Galgani[1,2,3]*, Eleni Tzempelikou[4a], Ioanna Kalantzi[4b], Anastasia Tsiola[4b], Manolis Tsapakis[4b], Paraskevi Pitta[4b], Chiara Esposito[5], Anastasia Tsotskou[6], Iordanis Magiopoulos[4b], Roberto Benavides[3], Tobias Steinhoff[3] and Steven A. Loiselle[1,7]

*corresponding author luisa.galgani@unisi.it

Affiliations

[1]Environmental Spectroscopy Group, Department of Biotechnology, Chemistry and Pharmacy, University of Siena, Italy

[2]Harbor Branch Oceanographic Institute of Florida Atlantic University, USA

[3]GEOMAR-Helmholtz Center for Ocean Research Kiel, Germany

[4a]Institute of Oceanography, Athens, [4b]Institute of Oceanography, Heraklion, [2c]Institute of Marine Biology Biotechnology & Aquaculture, Heraklion - Hellenic Centre for Marine Research, Greece.

[5]Department of Bioscience - Lake Ecology and WATEC, Center for Water Technology, Aarhus University, Denmark

[6]University of Western Macedonia, School of Agricultural Sciences, Department of Agriculture, Florina, Greece

[7]Consorzio Interuniversitario Nazionale per la Scienza e Tecnologia dei Materiali, Florence, Italy.

Keywords

Microplastics, pCO_2, pH, sea-surface microlayer, mesocosms, marine gel particles, dissolved and particulate organic matter

Abstract

Microplastics are substrates for microbial activity and can influence biomass production. This has potentially important implications at the sea-surface microlayer, the marine boundary layer that controls gas exchange with the atmosphere and where biologically produced organic compounds can accumulate. In the present study, we used large scale mesocosms (filled with 3 m^3 of seawater) to simulate future ocean scenarios. We explored microbial organic matter dynamics in the sea-surface microlayer in the presence and absence of microplastic contamination of the underlying water. Our study shows that microplastics increased both biomass production and enrichment of particulate carbohydrates and proteins in the sea-surface microlayer. Importantly, this resulted in a 3% reduction in the concentration of dissolved CO_2 in the underlying water. This reduction suggests direct and indirect impacts of microplastic pollution on the marine uptake of CO_2, by modifying the biogenic composition of the sea's boundary layer with the atmosphere.

Introduction

The transition layer between environments is home to many fundamental physical, chemical and biological processes. The sea-surface microlayer (SML) is a millimeter-sized interface between the ocean and the atmosphere (Liss & Duce, 2005). It plays an essential role in ocean-climate feedback by mediating air-sea gas exchange and marine aerosol emission (Wurl et al., 2017). The SML has distinctly different biogeochemical properties to its underlying seawater and it is enriched in organic matter, both dissolved organic matter (DOM) and particulate organic matter (POM), in particular carbohydrate-and protein-rich marine gel particles (Engel et al., 2017; Liss & Duce, 2005).

The two major classes of marine gel particles present in the SML are Transparent Exopolymer Particles (TEP) and Coomassie Stainable Particles (CSP). TEP and CSP give the SML its gel-like

composition which is prevalent in most parts of the ocean (Galgani et al., 2016; Wurl & Holmes, 2008) and support large and diversified microbial communities (Cunliffe & Murrell, 2009; Cunliffe et al., 2011), sensitive to local environmental and meteorological conditions (Rahlff et al., 2017; Zäncker et al., 2018). The enrichment of gel particles and their accompanying microbial life favors the creation of stable surface films that can influence the air-sea fluxes of oxygen and carbon dioxide (Calleja et al., 2013; Rahlff et al., 2019; Wurl et al., 2016).

Marine gel particles are derived from extracellular polymeric substances (EPS) released during microbial metabolic functions. EPS exist in a continuum of sizes, including colloidal as well as dissolved and particulate fractions (Decho & Gutierrez, 2017; Verdugo, 2012). TEP and CSP are considered a class of EPS (Decho & Gutierrez, 2017), larger than 0.4 µm in relation to the pore size of the filter used for their analysis (Engel, 2009).

The microbial release of exopolymers is enhanced on plastic surfaces (Michels et al., 2018), part of the carbon-rich substrates that make up the resulting biofilm (Lear et al., 2021; Zhao et al., 2021). The presence of microplastics in natural and artificial seawater can stimulate the microbial release of DOM, probably due to a higher substrate availability for microbial growth (Boldrini et al., 2021; Galgani et al., 2018). Likewise, both nanoparticles and microparticles can induce EPS secretion by phytoplankton (Santschi et al., 2021; Shiu et al., 2020). The increased production of organic matter around plastic particles can promote biogenic aggregates formation (Shiu et al., 2020). These aggregates can move to the deep ocean (Galgani & Loiselle, 2021; Michels et al., 2018) or remain in the SML (Galgani & Loiselle, 2019).

As plastic particles sustain niches for high microbial activity (Amaral-Zettler et al., 2020; Zettler et al., 2013), one central hypothesis of the present study is that higher concentration of microplastics in near surface conditions (< 3 m depths) stimulates a higher microbial production

of organic matter, adding on to the pool of organic compounds enriching the SML and thereby modify the air-sea gas exchange properties of this interface.

It has been recently shown that seawater exposed plastic debris directly release climate relevant gases like DMS (Savoca et al., 2016), methane and ethylene (Royer et al., 2018), suggesting that high concentrations of surface plastics may have a direct effect on water-air interactions. It has also been modeled that high concentrations of plastic can reduce the grazing pressure on phytoplankton in marine regions where nutrients are not a limiting factor, with subsequent anoxic conditions due to a cascade effect of initial high biomass production and degradation of the organic material (Kvale et al., 2021). Since much of the plastic at sea is concentrated in oligotrophic subtropical gyres (North Pacific, North Atlantic), it is expected that this additional carbon biomass on plastics offers an additional carbon source able to alter biogeochemical cycles (Zhao et al., 2021). Another central hypothesis of the present study was that higher microplastic concentrations would promote high biomass production in oligotrophic conditions.

To test both hypotheses, pseudo-marine conditions needed to be created, with well-defined and repeatable microplastic concentrations, but large enough to allow for aggregation, and for SML organic aggregates interaction with bulk water. Likewise, the experimental conditions should remain relatively stable over the medium term to allow for sampling of individual water masses with no mixing of waters with different microplastic concentrations. This was achieved by six large scale mesocosms, each filled with 3 m^3 of oligotrophic seawater from the Sea of Crete. Three of the mesocosms were amended with 30-µm diameter polystyrene microbeads (430 particles/L) and three were plastic-free control mesocosms (< 0.5 particles larger than 1 micron/L). The SML and bulk underlying water properties were compared over twelve days after the initial conditions, prior to microplastic addition, were controlled for uniformity.

Materials and methods

Mesocosms set up and SML sampling: Six mesocosms with a height of ~2.5 m and a diameter of 1.32 m made of transparent polyethylene were gravity-filled with 3-m^3 of coastal seawater pumped from below the surface (2 m) in the bay of Gournes (Sea of Crete). To ensure homogeneity of initial conditions, the water was divided equally in each of the six mesocosm and left overnight. The density of seawater during the experiment was 1.032 ± 0.001 g cm^{-3} with an average salinity of 41.4 ± 1.6 PSU. For the duration of the experiment (12 days), the mesocosms were kept in a 150 m^3 deep concrete tank with circulating seawater maintained at a constant temperature of 20±1 °C. Each mesocosm was protected by a clear PVC lid to avoid atmospheric contamination.-The first sampling (day 0) occurred the day after the mesocosms were filled. An aqueous solution of 30 µm diameter transparent polystyrene microbeads (Sigma-Aldrich, nr. 84135) with a density of 1.05 g cm^{-3} was added to three mesocosms (MP1-3) after the first sampling (day 1) for a concentration of 430 microplastic L^{-1}, corresponding to about 5.92 µg C L^{-1}. Polystyrene is a very abundant polymer found in oligotrophic marine areas (Pabortsava & Lampitt, 2020). Polystyrene beads and polyethylene walls have a negative surface charge at pH above 2.5 (Beneš & Paulenová, 1973), reducing the possibility of attraction between the two materials in experimental conditions. We choose not to clean the mesocosms walls from any possible biofilm formation: we believe that this external procedure could significantly interfere with the parameters measured and be more invasive than the effect of periphyton biofilm formed in a few days, which experimental studies show being negligible for larger radius mesocosm (Chung-Chi & Kemp, 2004). Recent experiments show biofilm formation on PE films after extended incubation times (> 60 and > 90 days) (Gupta & Devi, 2020; Han et al., 2020), not comparable to the present experiment.

114 The size range and concentration of polystyrene particles did not interfere with spectrophotometric
115 measurements of dissolved organic matter (Galgani et al., 2018; Galgani & Loiselle, 2019). While
116 a recent study has reported that virgin laboratory grade polymer and commercially available
117 polystyrene leaches dissolved organic carbon (DOC) in natural freshwater when exposed to dark
118 and light conditions (Lee et al., 2020), quantifiable DOC leaching was achieved at highly elevated
119 concentrations of 5 g L^{-1}, 10^6 times higher than the concentration used in the present study (6 x 10^{-6} g L^{-1}).
121 This microplastic size also allows for comparison to other studies on microplatsic influence on
122 marine biological processes like zooplankton ingestion (Cole et al., 2013; Cole et al., 2016) and
123 human health (Hwang et al., 2020).
124 Each mesocosm was continuously gently mixed through a centralized airlift system situated just
125 above the bottom surface to create a homogeneous distribution of the water, as described by Pitta
126 and colleagues (2016). The mixing system was the same in each mesocosm. Mesocosm set up,
127 manipulation, and sampling of the underlying water were conducted daily according to standard
128 methods for mesocosms studies performed at CretaCosmos facility
129 (https://www.aquacosm.eu/mesocosm/cretacosmos/) (Pitta et al., 2016; Tsiola, Tsagaraki, et al.,
130 2017). The sea-surface microlayer (SML) was sampled from each mesocosm early in the morning,
131 and prior to bulk water sampling on day 0, day 1, day 3, day 5, day 7, day 9 and day 10, to allow
132 a proper re-establishment of the surface film and minimized disturbance. The SML was sampled
133 contemporarily in each mesocosm with 30 cm x 30 cm silicate glass plates with an effective
134 sampling area of 1800 cm^2. Glass plates were inserted into the mesocosms perpendicular to the
135 surface and withdrawn at a controlled rate of ~ 6 cm s^{-1} as suggested by Carlson (Carlson, 1982).
136 The glass plate approach collects a thinner SML (~ 60–150 μm) when compared to, e.g., the

Garrett screen (150–300μm) (Garrett, 1965). The glass plate method allowed sampling of sufficient volume for analysis with a minimal dilution of the underlying water. The sample retained on both sides of the plates was removed with a wiper and poured into bottles with the aid of a funnel. The procedure was repeated until the necessary volume for analysis was obtained, tracking the exact amount of dips per mesocosm. The first sample was discarded and used to rinse the collecting bottle. Glass plates, collecting bottles, wipers and funnels were acid cleaned (HCl 10 %) and Milli-Q rinsed prior use. To avoid cross-contamination, the control mesocosms and the microplastic-treated mesocosms had different sampling equipment (glass plates, funnels, collection bottles, wipers).

The thickness (d, μm) of the sampled SML was estimated as:

$$d = V/(A\ x\ n) \quad (1)$$

where V is the SML volume collected, i.e., 60–140 mL, A is the sampling area of the glass plate (A = 1800 cm^2) and n is the number of dips. The apparent thickness of the SML ranged between 37 and 72 μm, with an overall mean of 54.7±9.0 μm in agreement to previous studies (Carlson, 1982; Engel et al., 2018; Galgani & Engel, 2016; Rahlff et al., 2019; Zäncker et al., 2017). The sampling thickness was similar for all mesocosms and sampling days. The samples were immediately processed in the laboratory within maximum 30 minutes after collection.

Dissolved Inorganic Carbon (DIC) and Total Alkalinity (TA) measurements: Following Dickson et al. (2007), seawater was drawn into 500 mL glass bottles using a tube to fill them from bottom to the top. Approximately half of the bottle volume was overflowed and a small head-space (approximately 1% of the bottle volume) was left to allow for water expansion. The samples were fixed by adding 100 μL saturated mercuric chloride ($HgCl_2$) solution thus preventing further biological activity and stored in the dark at room temperature until analysis. The DIC

measurements were performed using a coulometric technique with a SOMMA system (Johnson et al., 1998). The determination of TA was performed by potentiometric titration using a VINDTA system (Mintrop et al., 2000). Certified seawater samples were routinely measured to determine a precision estimated to 2.8µmol kg^{-1} for DIC and 1.8 µmol kg^{-1} for TA. ***Dissolved carbon dioxide estimates:*** The partial pressure of carbon dioxide in the mesocosms (pCO_2) as well as pH, CO_3^{2-}, HCO_3^- and CO_2 were calculated from DIC and TA at ambient temperature of 20±1°C and at sea-level pressure with the CO2SYS program (Pierrot et al., 2006) (https://cdiac.ess-dive.lbl.gov/ftp/co2sys/). We applied the equilibrium constants K1 and K2 of Lueker et al. (2000) as suggested by Dickson et al. (2007) and Orr et al. (2015) for a wider range of salinity and used a K_{SO4} value, the dissociation constant for HSO_4, of Dickson (1990).

Dissolved organic carbon (DOC) and chromophoric dissolved organic matter (CDOM): Samples for DOC were filtered immediately after sampling in duplicate through 0.2 µm polycarbonate membranes and stored cool (+4°C) in pre-combusted glass ampoules until analysis. Concentrations were determined using a Shimadzu TOC-V organic carbon analyser and following the high temperature catalytic oxidation method. The system was standardized prior to analysis using a potassium hydrogen phthalate standard solution. Each sample was injected 3 to 5 times and DOC concentrations were calculated from the average value of three replicates that yielded a relative standard deviation <2%. Analytical precision and accuracy were tested against Deep Atlantic Seawater Reference Material provided by the DOC-CRM program (University of Miami – D.A. Hansell, batch 16); measured values: 0.510-0.580 (n=10), certified value: 0.516-0.540. Drift correction of the DOC results was applied as needed.

Samples for CDOM were filtered immediately after collection in duplicates through 0.2 µm polyethersulfone syringe filters and stored cool (+4°C) in pre-combusted amber glass vials until

analysis, which was performed within 4 weeks. The CDOM absorbance spectrum was measured with a Lambda 10 ultraviolet-visible light (UV-Vis) Spectrophotometer (Perkin Elmer) from 210 to 750 nm at 960 nm/min, 1 nm wavelength resolution, and at room temperature (20ºC ± 2ºC). For each analysis, spectra were corrected for baseline, Milli-Q water absorbance and for scattering by subtracting the absorbance values at 730 nm. Absorption coefficients $a(\lambda)$ were calculated from absorbance values after Bricaud et al. (Bricaud et al., 1981). The CDOM absorption spectral slope S (nm^{-1}) was determined by linear regression of log-transformed absorption spectra against the wavelength (Bricaud et al., 1981):

$$a(\lambda) = a_0 e^{-S(\lambda-\lambda_0)} \quad (2)$$

With $a(\lambda_0)$ being the absorption coefficient at a reference wavelength λ_0. We used multiple 20-nm wavelength intervals in a stepwise (1 nm) linear regression analysis according to Loiselle et al. (Loiselle et al., 2009). Spectral slope correlates with changes in CDOM due to irradiation (photobleaching), and in the wavelength range 275-295, $S_{(275\text{-}295)}$ has been shown to be inversely related with DOM molecular weight (Helms et al., 2008).

Autotrophic and heterotrophic microorganisms: Abundances of autotrophic and heterotrophic microorganisms were measured by flow cytometry. Samples for heterotrophic bacteria were fixed with 25% 0.2 μm-filtered glutaraldehyde (0.5% final concentration), incubated at 4°C for 45 min, flash frozen in liquid nitrogen and stored at −80°C until analysis. Frozen samples were thawed at room temperature and sub-samples were stained for bacterial enumeration with the nucleic-acid stain SYBR Green I (final dilution 4×10^{-4} of the stock solution in Tris-EDTA buffer, pH = 8) and incubated for 10 min in the dark (Marie et al., 1997). Sample fluorescence signal to distinguish high and low DNA content cells. Samples for autotrophic microorganisms were not fixed and were

analysed without prior staining, based on their auto-fluorescence signals. A FACSCalibur™ flow cytometer (Becton Dickinson) was used following Tsiola et al. (2017).

Marine gels: Total area and numbers of gel particles were determined by optical microscopy (Engel, 2009). Ten to fifteen mL of sample were filtered using 0.2 µm Nuclepore membranes (Whatman) and stained with 1 mL Alcian Blue solution for polysaccharidic gels (Transparent Exopolymer Particles, TEP) and 1 mL Coomassie Brilliant Blue G solution for proteinaceous gels (Coomassie Stainable Particles, CSP). Filters were mounted onto Cytoclear® slides and stored at – 20ºC until microscopic analysis. For each slide, thirty images were taken randomly at 200x magnification with a light microscope equipped with a digital camera. The analysis of the cross-sectional area of marine gels was performed with an image analysis software (ImageJ, U.S. National Institutes of Health) and used to calculate the equivalent spherical diameter (ESD) of individual particles, particle number, volume and total area. The size frequency distribution of marine gel particles was determined according to their equivalent spherical diameter, described with a power function of the type:

$$\frac{dN}{d(d_p)} = k_p^{\delta} \quad (3)$$

with dN as the number of particles per unit volume in the size range d_p to $[d_p + d(d_p)]$, k a constant which depends on the concentrations of particles, and δ the slope ($\delta < 0$) describing the size distribution. A less negative δ implies an increase in the fraction of larger marine gels. k and δ were both derived from regressions of $\log[dN/d(d_p)]$ versus $\log[d_p]$ (Harlay et al., 2009; Mari & Burd, 1998; Mari & Kiørboe, 1996). The volume concentration of TEP and CSP refers to the mean volume of the particles > 0.2 µm (membrane pore size cutoff); changes in this parameter indicate modifications in particle dynamics such as aggregation/disaggregation processes.

Since TEP are considered fractal aggregates, the volume and the carbon content of these marine gel particles are assumed to be proportional to r^D, with r being the equivalent spherical radius (µm) and D the fractal scaling dimension associated with the size-distribution of marine gels (Engel, 2009; Mari & Burd, 1998; Mari & Kiørboe, 1996). TEP carbon content (TEP-C, expressed in µg L^{-1}) was determined from marine gel size spectra according to Mari (Mari, 1999) and Engel (2009):

$$\text{TEP-C } [\mu g\ L^{-1}] = 0.25 \times 10^{-6}\ r^D \quad (4)$$

With D = - 2.55

Enrichment Factors*:* To determine the enrichment or the depletion of each parameter analysed in the SML compared to the underlying water, we determined the Enrichment Factor (EF), defined as:

$$EF = ([X]_\mu / [X]_b) \quad (5)$$

With $[X]_\mu$, $[X]_b$ the concentration of the specific parameter in the SML (µ) or underlying water (b) (Liss & Duce, 2005). An EF = 1 indicates that SML and underlying water values are similar, thus no enrichment or depletion in the SML. While bubbling may have promoted the enrichment of certain compounds in the SML, this process occurred in all mesocosms thus the influence of the airlift mixing system in the comparison of the dynamics of plastic free versus plastic enriched treatments is negligible.

Data analysis and statistics: To highlight the treatment effect (microplastic addition) and avoid the temporal variability, we calculated the normalized anomaly y_{ij} of each mesocosm (j) per day (i = 0, . . ., 11) from the overall daily mean of the mesocosms $\overline{y}_i = \frac{1}{6}\sum_j^6 (x_j)_i$ following a procedure often applied in mesocosms studies (Endres et al., 2014; Engel et al., 2013):

$$y_{ij} = (x_{ij} - \overline{y}_i)/\overline{y}_i \quad (6)$$

Differences between control and treated mesocosms were determined by two-tailed unpaired t-tests and Mann-Whitney tests on normalized anomalies, depending on the distribution of the data. Repeated Measures Two-Way ANOVA and Mixed Effects Model (REML) were also used to analyse temporal variations between the control and microplastic treated mesocosms, the latter used in case of missing observations. This method is widely used to analyse data from mesocosms experiments (Dimitriou et al., 2017; Rahav et al., 2016). The fixed factor considered is the treatment (microplastics addition / control) and the random effect is time (days). Correlations among parameters were determined by Multiple Linear Regression and Spearman correlation analysis. Statistical significance was accepted for $p < 0.05$ and considering a Bonferroni correction for multiple comparisons. All statistical tests were performed with Prism 8.02 (GraphPad Software, San Diego, CA, USA) and Minitab18 (Minitab Inc., USA).

Results

An earlier study reported an increase in the production of POM and marine gels in the bulk waters of the plastic-amended mesocosms with respect to the plastic-free controls (Galgani et al., 2019). In the present study, we explore differences in the composition of the SML and the possible influence of different SML compositions on the pCO_2 of the underlying bulk water. The SML was analysed for marine gel particles (TEP and CSP), autotrophic and heterotrophic microbial organisms, and dissolved organic matter parameters: Dissolved Organic Carbon, DOC, Chromophoric Dissolved Organic Matter, CDOM, and spectral slope. Salinity, total alkalinity and dissolved inorganic carbon (DIC) were measured from the underlying water and *in-situ* pCO_2, pH, CO_3^{2-}, HCO_3^- and CO_2 were retrieved accordingly. In the following paragraphs, all parameters described refer to the SML, except where specified. Biogeochemical processes and relevant data

of the underlying water are described in a previous publication (Galgani et al., 2019) and were not the focus of this study.

Sea surface microlayer dynamics and underlying water pCO_2

Microplastic-amended mesocosms (MP) had significantly lower values of pCO_2 in the underlying water and higher pH compared to control mesocosms (Figure 1). Mean values of pCO_2 in the MP treatments were 3% lower than those found in control mesocosms, corresponding to an increase of 0.14% in pH units (Table 1). Total alkalinity (TA) and dissolved inorganic carbon (DIC) were also significantly higher in the underlying water of MP treatments (Figures 2 and S1). Similar differences were found for estimated concentrations of CO_3^{2-} and CO_2, with higher CO_3^{2-} in MP treatments (Figure 2).

Higher concentrations of both polysaccharidic TEP and proteinaceous CSP were measured in the SML of the MP treated mesocosms (Figure 1, Table 1). An 30% increase in TEP and relative carbon content (TEP-C) along with higher concentrations and particle abundances of both marine gels occurred in the SML of the MP mesocosms, with a mean±SEM (standard error of means) TEP-C of 424.8±58.5 µg C L^{-1} compared to 324.3±42.9 µg C L^{-1} in control mesocosms (Figure 1). This was accompanied by a 1% increase in *Synechococcus*, and by a 23% increase of high-DNA containing cells in the SML (Figures 1 and S2, Table 1), likely to be the main source of TEP for the whole system. In the underlying water of the mesocosms, an initial (and rapidly declined) phytoplankton bloom was attributed to the presence of autotrophic picoeukaryotes, while *Synechococcus* growth showed a constant increase and represented the dominant species in the mesocosms. This was expected as this species dominates in the oligotrophic waters of the Sea of Crete at this time of the year (Galgani et al., 2019). Heterotrophic bacteria concentrations in the SML were similar in MP and control mesocosms, and significant differences were observed over

time rather than across treatments (Figure S2, Table 1). Their concentrations were negatively correlated to those of *Synechoccous*, indicating a potential competition within the highly dynamic environment of the SML (Spearman r =-0.40, p=0.015, n=37). Alternating influence of primary and secondary production in the SML was also evidenced in the dynamics of the spectral slope $S_{275\text{-}295}$ of the chromophoric dissolved organic matter (CDOM) pool. Higher $S_{275\text{-}295}$ is associated to lower molecular weight CDOM often resulting from degradation processes, while lower $S_{275\text{-}295}$ characterizes the production of higher molecular weight CDOM (Helms et al., 2008).

While DOC and CDOM measured as the absorption coefficient at 355 nm were similar between control and MP mesocosms and significant variations were observed over time (Table 1, Figure S3), $S_{275\text{-}295}$ instead was higher in the SML of MP mesocosms (Table 1, Figure S3) confirming that there were significant differences in the DOM production and degradation processes between treatments. In the SML, we observed a strong negative correlation between *Synechococcus* and $S_{275\text{-}295}$ (Table 2), and a weaker positive correlation between heterotrophic bacteria and $S_{275\text{-}295}$. $S_{275\text{-}295}$ was positively correlated to CSP ($mm^2\ L^{-1}$), DOC and pCO_2 (Table 2) suggesting different production dynamics of CSP with respect to TEP and linking CSP concentration to organic matter degradation. In the SML, the amount of TEP-C was weakly related to the abundance of *Synechococcus* (Linear Regression R^2=0.12, p = 0.03) suggesting a local source (i.e., within the SML) of fresh biological production for this class of marine gel compounds. A positive correlation between DOC and $S_{275\text{-}295}$ suggested that the pool of DOC in the SML of the mesocosms is mostly composed of degraded or reworked material, and unlikely linked to a fresh biomass production.

Most importantly, we observed significant correlations between the pCO_2 in the underlying water (as well as pH, TA, DIC, CO_3^{2-} and CO_2) with the concentration of TEP-C and *Synechococcus* cells in the SML (Table 3). pCO_2 decreased with increasing TEP concentration and carbon content

(Figure S4a). Instead, CSP in the SML had the opposite relationship with pCO_2 with respect to TEP (Figure 3). This was further demonstrated in the linear relationship between pCO_2 and gel concentrations (Equation 7):

$$pCO_2\ [\mu atm] = 413.189 - 0.0509\ TEP\ [mm^2\ L^{-1}] + 0.04708\ CSP\ [mm^2\ L^{-1}] \quad (7)$$

$R^2 = 0.38,\ p < 0.001,\ F=11.98$

It should be noted that underlying water TEP and CSP concentrations from the same experiment did not show any relation to pCO_2. Together with SML gel concentrations, pCO_2 in the underlying water was related to SML $S_{275\text{-}295}$ and SML *Synechococcus* abundance (Figures S4b, S4c and Tables 2 and 3), indicating the relationship of pCO_2 to different phases of organic matter cycling.

Sea surface microlayer enrichment and relation to underlying water parameters

In this experiment, the SML represented an enriched environment with respect to the bulk water conditions (Figure 4). *Synechococcus* in the SML was strongly related to the underlying water cell abundances (Spearman r = 0.945, $p < 0.0001$, n =39), as well as the amount of CDOM (Spearman r = 0.859, $p < 0.0001$, n =42), the latter pointing to similar dynamics in DOM turnover between SML and underlying water. TEP concentration ($mm^2\ L^{-1}$) in the SML also showed a low but significant relation to underlying water TEP to some extent (Spearman r = 0.359, p =0.0197, n =42), confirming that most of the TEP variability in the SML was associated to *Synechococcus* cell abundances.

Particularly high enrichment factors were observed for marine gels in the SML in all mesocosms, as expected. However, the enrichment factors for TEP and CSP were significantly higher in the MP mesocosms with respect to plastic-free controls (Figure 5, Table S1) indicating an increased accumulation of these gels in the SML of the mesocosms where plastic was added.

It should be noted that the concentration of plastic particles used in this study is higher than typical marine conditions and more similar to those of impacted coastal areas and projections of future conditions. Plastic production is expected to double in the next decades and in the absence of efficient management practices, will likely increase the amount of plastic in our oceans (Geyer et al., 2017). High concentrations of microplastics (10^5 particles m^{-3}) have been already found in a Swedish harbour in proximity of a plastic manufacture plant (Lindgren et al., 2016).

Discussion

The twelve-day experiment coincided with a *Synechococcus* bloom phase in all six mesocosms, during which autotrophic production of particulate organic matter prevailed over heterotrophic production. In the MP mesocosms there was an increased abundance of *Synechococcus* in the underlying water, which dominated over autotrophic picoeukaryotes cell numbers by an order of magnitude (Galgani et al., 2019). Microbial attachment on particles is a general phenomenon in aquatic ecosystems (Paerl, 1975) and microplastics may serve as a physical support for different microorganisms (Zettler et al., 2013; Zhao et al., 2021) creating hot spots of high metabolic activity (Dang & Lovell, 2015).

Synechococcus is an important primary producer in the Sea of Crete and a known TEP producer also in nutrient-limiting conditions (Deng et al., 2016; Ortega-Retuerta et al., 2019). Globally, *Synechococcus* contributes to 21% of total CO_2 fixation (Jardillier et al., 2010).

We hypothesize that two concurrent processes led to the increased accumulation of TEP in the surface microlayer of the mesocosms containing MPs. Firstly, MP related increases in *Synechococcus* production led to increased TEP accumulation in the underlying water and enrichment in the SML. The relationship between underlying water and SML gel particles is not novel in field (Engel & Galgani, 2016) and mesocosms studies (Galgani et al., 2014). Secondly,

363 *Synechococcus* cells can produce TEP directly in the SML (Yue et al., 2018) and their increased
364 concentration in the SML in the mesocosms containing MPs was an additional source for TEP
365 accumulation.
366 In the ocean, TEP aggregation is proved to be a sink for marine carbon (Engel et al., 2004) and
367 TEP production as a response to increased CO_2 has been demonstrated for natural plankton
368 communities (Engel, 2002). It has also been shown that microbial activity in the sea-surface
369 microlayer can control the exchange rate of atmospheric CO_2 (Calleja et al., 2005), and in our
370 experiment, TEP accumulation in the SML of the MP mesocosms may have served as a sink for
371 CO_2 as described in equation (7).
372 To further support this difference, DIC partitioning in the underlying water of MP mesocosms had
373 higher CO_3^{2-} and lower CO_2 concentrations.
374 *Synechococcus* has also been associated to "whiting" events in marine and lakes environments
375 (Dittrich et al., 2003; Thompson et al., 1997). Whiting events occur when carbonates of biogenic
376 origin are precipitated by microorganisms like cyanobacteria through photo-and chemosynthetic
377 autotrophy in the presence of Mg and Ca counterions (Dittrich et al., 2003; Thompson, 2000;
378 Thompson et al., 1997). Many bacteria species are implicated in $CaCO_3$ precipitation, which
379 represents a potential mechanism for CO_2 sequestration and generally occurs at high pH, during
380 active photosynthesis, and when DIC is limiting, such as after a bloom (Callieri, 2017). During the
381 twelve-day experiment, the highest abundance of *Synechococcus* in the SML and underlying water
382 appeared after the picoeukaryote and heterotrophic blooms (Galgani et al., 2019), corresponding
383 to a migration and enrichment of organic compounds to the SML.
384 In particular, the enrichment of organic particles (i.e. TEP and CSP) in the SML of MP mesocosms
385 led to the establishment of a highly enriched surface film, potentially able to modify gas exchange

between the mesocosms and the surrounding atmosphere. The different partitioning of DIC between CO_3^{2-} and CO_2 in MP treatments confirms an increased autotrophy in MP mesocosms that led to lower pCO_2 beneath. In control mesocosms, heterotrophy did not increase, rather, autotrophic production was less as additional microplastic substrates for growth and metabolism were missing. This led to an overall lower production of marine gels in the underlying water and in the SML, resulting in a less enriched surface film and an increased exchange of atmospheric CO_2 at the air-sea interface. This is similar to the presence of surfactants in the sea-surface microlayer, where the resulting laminar diffusion layer reduces gas transfer (Frew, 1997). Some biogenic surfactants and surface slicks carrying a high microbial biomass can reduce air-sea CO_2 exchange by 15% to 19% (Mustaffa et al., 2020; Wurl et al., 2016).

While initially pCO_2 concentration might have been lower in the MP mesocosms, we should note that SML enrichment does not only limit the exchange of atmospheric CO_2, but also that of oxygen across the air-sea interface. In the post-bloom phase dominated by the heterotrophic remineralization of organic matter, CO_2 is put back into the system through microbial respiration, while oxygen concentrations are reduced. This may be especially important in coastal, shallow and semi-enclosed marine areas affected by plastic and other types of organic or nutrient pollution that favour high autotrophic biomass production. In areas where zooplankton feed on plastic particles because of high plastic concentration, grazing pressure on primary producers is reduced, further increasing autotrophic biomass in eutrophic waters, where the subsequent remineralization of organic matter can further reduce oxygen concentrations (Kvale et al., 2021).

Our study shows that microplastics can increase the accumulation of marine gel particles in the SML by a 25-30% compared to plastic-free conditions. By using large scale mesocosms, it was possible to explore daily changes in SML formation and the resulting impact on the underlying

409 water pCO_2. This supports a better understanding of localized anoxic or hypoxic zones often
410 observed in estuarine and upwelling areas where the SML plays an essential role in air-sea gas
411 exchange (Engel & Galgani, 2016; Hepach et al., 2016; Upstill-Goddard, 2006) and where marine
412 plastisphere communities can have direct effect on the concentration of N_2O and CO_2 (Cornejo-
413 D'Ottone et al., 2020; Su et al., 2022).
414 While this method demonstrated the indirect effect of plastics on seawater pCO_2 concentration
415 through the SML, another effect that should be considered is the direct impact on the production
416 and response of marine gels in the SML. TEP and CSP are distinct, insoluble macromolecules
417 derived from the aggregation and annealing of DOM polymeric precursors produced during
418 microbial growth and metabolism (Cisternas-Novoa et al., 2015; Engel, 2009; Thornton, 2018;
419 Thornton et al., 2016). TEP concentrations in the SML were only partly related to those of the
420 underlying water, indicating that an additional source of TEP may be the SML itself through the
421 microbial activity of *Synechococcus*. As such, the SML may act as a direct sink of atmospheric
422 CO_2. CSP instead seemed to be more clearly related to the degradation of organic matter present
423 in the SML, as CDOM and $S_{275\text{-}295}$ measurements indicated their higher lability and rapid turnover
424 (Thornton, 2018). This creates a pool of organic matter in the SML that is completely independent
425 from underlying water processes, a phenomenon observed in highly productive marine regions
426 (Galgani & Engel, 2016; Zäncker et al., 2017).
427 The present mesocosm study shows an important new impact of plastic pollution on marine carbon
428 biogeochemistry that directly affects processes at the air-sea boundary layer. The increased
429 production and accumulation of these two different classes of marine gels in the SML represent an
430 important mechanism regulating air sea gas exchange, both indirectly through an enriched surface
431 film, as well as directly as the site for high remineralization of organic matter.

Conclusions

An increasing number of studies suggests that plastic pollution influences the marine biological pump and the ocean's capability to store the increasing atmospheric amounts of anthropogenic carbon dioxide (Galgani & Loiselle, 2021; Kvale et al., 2021; Shen et al., 2020). Our results show the impact of plastic pollution at the very surface of the ocean, with direct and indirect mechanisms that control the ocean CO_2 exchange with the atmosphere. Further efforts should be made to explore these mechanisms across different marine conditions and autotrophic species. Clearly, plastic pollution impacts on marine biogeochemistry go well beyond that explored to date, and should be included in international agreements for their potential effects on the functionality of the ocean carbon sink (Cooley et al., 2019).

Acknowledgements

We greatly acknowledge G. Piperakis for the setting up of the mesocosms and for his technical assistance throughout the experiment. K. Mylona, I. Santi, S, Zivanovic, E. Dafnomili, S. Diliberto, and A. Loiselle are greatly acknowledged for technical support.

Author contributions: Author contributions: LG designed the experiment in consultation with SAL, MT and PP, analysed the data in consultation with SAL and wrote the manuscript. LG, ET, IK, AT, MT, PP, CE, ATs, IM, and SAL contributed to set up and experiment running, samples analysis and manuscript editing. RB and TS contributed to samples analysis and manuscript editing.

Funding: This work received funding from the European Union's Horizon 2020 Research and Innovation Programme under the Marie Skłodowska-Curie grant agreement No. 702747 – *POSEIDOMM*, to L. Galgani.

Competing Interests: The authors declare no competing interests.

Data availability: all data will be made available on an open repository after publication in conformity with the requirements of all Horizon 2020 funded research projects.

References

Amaral-Zettler, L. A., Zettler, E. R., & Mincer, T. J. (2020). Ecology of the plastisphere. *Nat. Rev. Microbiol.*, *18*(3), 139-151. https://doi.org/10.1038/s41579-019-0308-0

Beneš, P., & Paulenová, M. (1973). Surface charge and adsorption properties of polyethylene in aqueous solutions of inorganic electrolytes. *Kolloid-Zeitschrift und Zeitschrift für Polymere*, *251*(10), 766-771. https://doi.org/10.1007/BF01499104

Boldrini, A., Galgani, L., Consumi, M., & Loiselle, S. A. (2021). Microplastics Contamination versus Inorganic Particles: Effects on the Dynamics of Marine Dissolved Organic Matter. *Environments*, *8*(3), 21. https://doi.org/https://doi.org/10.3390/environments8030021

Bricaud, A., Morel, A., & Prieur, L. (1981). Absorption by dissolved organic matter of the sea (yellow substance) in the UV and visible domains. *Limnol. Oceanogr.*, *26*, 43-53. https://doi.org/https://doi.org/10.4319/lo.1981.26.1.0043

Calleja, M. L., Duarte, C. M., Álvarez, M., Vaquer-Sunyer, R., Agustí, S., & Herndl, G. J. (2013). Prevalence of strong vertical CO2 and O2 variability in the top meters of the ocean. *Global Biogeochem. Cycles*, *27*(3), 941-949. https://doi.org/10.1002/gbc.20081

Calleja, M. L., Duarte, C. M., Navarro, N., & Agustí, S. (2005). Control of air-sea CO2 disequilibria in the subtropical NE Atlantic by planktonic metabolism under the ocean skin. *Geophysical Research Letters*, *32*(8). https://doi.org/https://doi.org/10.1029/2004GL022120

Callieri, C. (2017). Synechococcus plasticity under environmental changes. *FEMS Microbiol. Lett.*, *364*(23). https://doi.org/10.1093/femsle/fnx229

Carlson, D. J. (1982). Phytoplankton in marine surface microlayers. *Can. J. Microbiol.*, *28*(11), 1226-1234. https://doi.org/10.1139/m82-183

Chung-Chi, C., & Kemp, W. M. (2004). Periphyton communities in experimental marine ecosystems: scaling the effects of removal from container walls. *Marine Ecology Progress Series*, *271*, 27-41. https://www.int-res.com/abstracts/meps/v271/p27-41/

Cisternas-Novoa, C., Lee, C., & Engel, A. (2015). Transparent exopolymer particles (TEP) and Coomassie stainable particles (CSP): Differences between their origin and vertical distributions in the ocean. *Mar. Chem.*, *175*, 56-71. https://doi.org/https://doi.org/10.1016/j.marchem.2015.03.009

Cole, M., Lindeque, P., Fileman, E., Halsband, C., Goodhead, R., Moger, J., & Galloway, T. S. (2013). Microplastic Ingestion by Zooplankton. *Environ. Sci. Technol.*, *47*(12), 6646-6655. https://doi.org/10.1021/es400663f

Cole, M., Lindeque, P. K., Fileman, E., Clark, J., Lewis, C., Halsband, C., & Galloway, T. S. (2016). Microplastics Alter the Properties and Sinking Rates of Zooplankton Faecal Pellets. *Environ. Sci. Technol.*, *50*(6), 3239-3246. https://doi.org/10.1021/acs.est.5b05905

Cooley, S. R., Bello, B., Bodansky, D., Mansell, A., Merkl, A., Purvis, N., Ruffo, S., Taraska, G., Zivian, A., & Leonard, G. H. (2019). Overlooked ocean strategies to address climate change. *Glob. Environ. Change*, *59*, 101968. https://doi.org/https://doi.org/10.1016/j.gloenvcha.2019.101968

494 Cornejo-D'Ottone, M., Molina, V., Pavez, J., & Silva, N. (2020). Greenhouse gas cycling by the
495 plastisphere: The sleeper issue of plastic pollution. *Chemosphere, 246*, 125709.
496 https://doi.org/https://doi.org/10.1016/j.chemosphere.2019.125709

497 Cunliffe, M., & Murrell, J. C. (2009). Eukarya 18S rRNA gene diversity in the sea surface microlayer:
498 implications for the structure of the neustonic microbial loop. *ISME J.*, *4*(3), 455-458.
499 https://doi.org/10.1038/ismej.2009.133

500 Cunliffe, M., Upstill-Goddard, R. C., & Murrell, J. C. (2011). Microbiology of aquatic surface microlayers.
501 *FEMS Microbiol. Rev.*, *35*(2), 233-246. https://doi.org/10.1111/j.1574-6976.2010.00246.x

502 Dang, H., & Lovell, C. R. (2015). Microbial Surface Colonization and Biofilm Development in Marine
503 Environments. *Microbiol. Mol. Biol. Rev.: MMBR*, *80*(1), 91-138.
504 https://doi.org/10.1128/MMBR.00037-15

505 Decho, A. W., & Gutierrez, T. (2017). Microbial Extracellular Polymeric Substances (EPSs) in Ocean
506 Systems. *Frontiers in Microbiology*, *8*. https://doi.org/10.3389/fmicb.2017.00922

507 Deng, W., Cruz, B. N., & Neuer, S. (2016). Effects of nutrient limitation on cell growth, TEP production
508 and aggregate formation of marine Synechococcus. *Aquat. Microb. Ecol.*, *78*(1), 39-49.
509 https://www.int-res.com/abstracts/ame/v78/n1/p39-49/

510 Dickson, A. G. (1990). Standard potential of the reaction: AgCl(s) + 12H2(g) = Ag(s) + HCl(aq), and and
511 the standard acidity constant of the ion HSO4− in synthetic sea water from 273.15 to 318.15 K. *J.*
512 *Chem. Thermodyn.*, *22*(2), 113-127. https://doi.org/https://doi.org/10.1016/0021-9614(90)90074-Z

513 Dickson, A. G., Sabine, C. L., & Christian, J. R. E. (2007). *Guide to Best Practices for Ocean CO2*
514 *Measurements*. PICES Special Publication 3, 191 pp. https://www.ncei.noaa.gov/access/ocean-
515 carbon-acidification-data-system/oceans/Handbook_2007.html

516 Dimitriou, P. D., Papageorgiou, N., Geropoulos, A., Kalogeropoulou, V., Moraitis, M., Santi, I.,
517 Tsikopoulou, I., Pitta, P., & Karakassis, I. (2017). A novel mesocosm setup for benthic-pelagic
518 coupling experiments. *Limnology and Oceanography: Methods*, *15*(4), 349-362.
519 https://doi.org/https://doi.org/10.1002/lom3.10163

520 Dittrich, M., Müller, B., Mavrocordatos, D., & Wehrli, B. (2003). Induced Calcite Precipitation by
521 Cyanobacterium Synechococcus. *Acta Hydrochim. Hydrobiol.*, *31*(2), 162-169.
522 https://doi.org/https://doi.org/10.1002/aheh.200300486

523 Endres, S., Galgani, L., Riebesell, U., Schulz, K.-G., & Engel, A. (2014). Stimulated Bacterial Growth
524 under Elevated pCO2: Results from an Off-Shore Mesocosm Study. *PLOS ONE*, *9*(6), e99228.
525 https://doi.org/10.1371/journal.pone.0099228

526 Engel, A. (2002). Direct relationship between CO2 uptake and transparent exopolymer particles production
527 in natural phytoplankton. *J. Plankton Res.*, *24*(1), 49-53. https://doi.org/10.1093/plankt/24.1.49

528 Engel, A. (2009). Determination of Marine Gel Particles. In O. E. Wurl (Ed.), *Practical Guidelines for the*
529 *Analysis of Seawater*. CRC Press. https://doi.org/doi:10.1201/9781420073072.ch7

530 Engel, A., Bange, H. W., Cunliffe, M., Burrows, S. M., Friedrichs, G., Galgani, L., Herrmann, H., Hertkorn,
531 N., Johnson, M., Liss, P. S., Quinn, P. K., Schartau, M., Soloviev, A., Stolle, C., Upstill-Goddard,
532 R. C., van Pinxteren, M., & Zäncker, B. (2017). The Ocean's Vital Skin: Toward an Integrated
533 Understanding of the Sea Surface Microlayer. *Front. Mar. Sci.*, *4*(165).
534 https://doi.org/10.3389/fmars.2017.00165

Engel, A., Borchard, C., Piontek, J., Schulz, K. G., Riebesell, U., & Bellerby, R. (2013). CO_2 increases ^{14}C primary production in an Arctic plankton community. *Biogeosciences*, *10*(3), 1291-1308. https://doi.org/10.5194/bg-10-1291-2013

Engel, A., & Galgani, L. (2016). The organic sea-surface microlayer in the upwelling region off the coast of Peru and potential implications for air–sea exchange processes. *Biogeosciences*, *13*(4), 989-1007. https://doi.org/10.5194/bg-13-989-2016

Engel, A., Sperling, M., Sun, C., Grosse, J., & Friedrichs, G. (2018). Organic Matter in the Surface Microlayer: Insights From a Wind Wave Channel Experiment. *Front. Mar. Sci.*, *5*(182). https://doi.org/10.3389/fmars.2018.00182

Engel, A., Thoms, S., Riebesell, U., Rochelle-Newall, E., & Zondervan, I. (2004). Polysaccharide aggregation as a potential sink of marine dissolved organic carbon. *Nature*, *428*(6986), 929-932. https://doi.org/https://doi.org/10.1038/nature02453

Frew, N. M. (1997). The role of organic films in air–sea gas exchange. In P. S. Liss & R. A. Duce (Eds.), *The Sea Surface and Global Change* (pp. 121-172). Cambridge University Press. https://doi.org/DOI: 10.1017/CBO9780511525025.006

Galgani, L., & Engel, A. (2016). Changes in optical characteristics of surface microlayers hint to photochemically and microbially mediated DOM turnover in the upwelling region off the coast of Peru. *Biogeosciences*, *13*(8), 2453-2473. https://doi.org/10.5194/bg-13-2453-2016

Galgani, L., Engel, A., Rossi, C., Donati, A., & Loiselle, S. A. (2018). Polystyrene microplastics increase microbial release of marine Chromophoric Dissolved Organic Matter in microcosm experiments. *Sci. Rep.*, *8*(1), 14635. https://doi.org/10.1038/s41598-018-32805-4

Galgani, L., & Loiselle, S. A. (2019). Plastic Accumulation in the Sea Surface Microlayer: An Experiment-Based Perspective for Future Studies. *Geosciences*, *9*. https://doi.org/https://doi.org/10.3390/geosciences9020066

Galgani, L., & Loiselle, S. A. (2021). Plastic pollution impacts on marine carbon biogeochemistry. *Environ. Pollut.*, *268*, 115598. https://doi.org/https://doi.org/10.1016/j.envpol.2020.115598

Galgani, L., Piontek, J., & Engel, A. (2016). Biopolymers form a gelatinous microlayer at the air-sea interface when Arctic sea ice melts. *Sci. Rep.* , *6*, 29465.

Galgani, L., Stolle, C., Endres, S., Schulz, K. G., & Engel, A. (2014). Effects of ocean acidification on the biogenic composition of the sea-surface microlayer: Results from a mesocosm study. *Journal of Geophysical Research: Oceans*, *119*(11), 7911-7924. https://doi.org/10.1002/2014jc010188

Galgani, L., Tsapakis, M., Pitta, P., Tsiola, A., Tzempelikou, E., Kalantzi, I., Esposito, C., Loiselle, A., Tsotskou, A., Zivanovic, S., Dafnomili, E., Diliberto, S., Mylona, K., Magiopoulos, I., Zeri, C., Pitta, E., & Loiselle, S. A. (2019). Microplastics increase the marine production of particulate forms of organic matter. *Environ. Res. Lett.* https://doi.org/https://doi.org/10.1088/1748-9326/ab59ca

Garrett, W. D. (1965). Collection of Slick-forming Materials from the Sea Surface. *Limnol. Oceanogr.*, *10*, 602-605. https://doi.org/https://doi.org/10.4319/lo.1965.10.4.0602

Geyer, R., Jambeck, J. R., & Law, K. L. (2017). Production, use, and fate of all plastics ever made. *Sci. Adv.* *3*(7). http://advances.sciencemag.org/content/3/7/e1700782.abstract

Gupta, K. K., & Devi, D. (2020). Characteristics investigation on biofilm formation and biodegradation activities of Pseudomonas aeruginosa strain ISJ14 colonizing low density polyethylene (LDPE) surface. *Heliyon*, *6*(7), e04398. https://doi.org/https://doi.org/10.1016/j.heliyon.2020.e04398

Han, Y. N., Wei, M., Han, F., Fang, C., Wang, D., Zhong, Y. J., Guo, C. L., Shi, X. Y., Xie, Z. K., & Li, F. M. (2020). Greater Biofilm Formation and Increased Biodegradation of Polyethylene Film by a Microbial Consortium of Arthrobacter sp. and Streptomyces sp. *Microorganisms*, *8*(12). https://doi.org/10.3390/microorganisms8121979

Harlay, J., De Bodt, C., Engel, A., Jansen, S., d,ÄôHoop, Q., Piontek, J., Van Oostende, N., Groom, S., Sabbe, K., & Chou, L. (2009). Abundance and size distribution of transparent exopolymer particles (TEP) in a coccolithophorid bloom in the northern Bay of Biscay. *Deep Sea Res. Part I Oceanogr. Res. Pap.*, *56*(8), 1251-1265. https://doi.org/10.1016/j.dsr.2009.01.014

Helms, J. R., Stubbins, A., Ritchie, J. D., Minor, E. C., Kieber, D. J., & Mopper, K. (2008). Absorption spectral slopes and slope ratios as indicators of molecular weight, source, and photobleaching of chromophoric dissolved organic matter. *Limnol. Oceanogr.*, *53*(3), 955-969. https://doi.org/https://doi.org/10.4319/lo.2008.53.3.0955

Hepach, H., Quack, B., Tegtmeier, S., Engel, A., Bracher, A., Fuhlbrügge, S., Galgani, L., Atlas, E. L., Lampel, J., Frieß, U., & Krüger, K. (2016). Biogenic halocarbons from the Peruvian upwelling region as tropospheric halogen source. *Atmos. Chem. Phys.*, *16*(18), 12219-12237. https://doi.org/10.5194/acp-16-12219-2016

Hwang, J., Choi, D., Han, S., Jung, S. Y., Choi, J., & Hong, J. (2020). Potential toxicity of polystyrene microplastic particles. *Sci. Rep.*, *10*(1), 7391. https://doi.org/10.1038/s41598-020-64464-9

Jardillier, L., Zubkov, M. V., Pearman, J., & Scanlan, D. J. (2010). Significant CO2 fixation by small prymnesiophytes in the subtropical and tropical northeast Atlantic Ocean. *ISME J.*, *4*(9), 1180-1192. https://doi.org/10.1038/ismej.2010.36

Johnson, K. M., Dickson, A. G., Eischeid, G., Goyet, C., Guenther, P., Key, R. M., Millero, F. J., Purkerson, D., Sabine, C. L., Schottle, R. G., Wallace, D. W. R., Wilke, R. J., & Winn, C. D. (1998). Coulometric total carbon dioxide analysis for marine studies: assessment of the quality of total inorganic carbon measurements made during the US Indian Ocean CO2 Survey 1994–1996. *Mar. Chem.*, *63*(1), 21-37. https://doi.org/https://doi.org/10.1016/S0304-4203(98)00048-6

Kvale, K., Prowe, A. E. F., Chien, C. T., Landolfi, A., & Oschlies, A. (2021). Zooplankton grazing of microplastic can accelerate global loss of ocean oxygen. *Nat. Commun.* , *12*(1), 2358. https://doi.org/10.1038/s41467-021-22554-w

Lear, G., Kingsbury, J. M., Franchini, S., Gambarini, V., Maday, S. D. M., Wallbank, J. A., Weaver, L., & Pantos, O. (2021). Plastics and the microbiome: impacts and solutions. *Environmental Microbiome*, *16*(1), 2. https://doi.org/10.1186/s40793-020-00371-w

Lee, Y. K., Murphy, K. R., & Hur, J. (2020). Fluorescence Signatures of Dissolved Organic Matter Leached from Microplastics: Polymers and Additives. *Environ. Sci. Technol.*, *54*(19), 11905-11914. https://doi.org/10.1021/acs.est.0c00942

Lindgren, J. F., Wilewska-Bien, M., Granhag, L., Andersson, K., & Eriksson, K. M. (2016). Discharges to the Sea. In K. Andersson, S. Brynolf, J. F. Lindgren, & M. Wilewska-Bien (Eds.), *Shipping and the Environment : Improving Environmental Performance in Marine Transportation* (pp. 125-168). Springer Berlin Heidelberg. https://doi.org/10.1007/978-3-662-49045-7_4

Liss, P. S., & Duce, R. A. (2005). *The Sea Surface and Global Change*. Cambridge University Press. https://doi.org/doi:10.1017/CBO9780511525025

Loiselle, S. A., Bracchini, L., Dattilo, A. M., Ricci, M., Tognazzi, A., Cózar, A., & Rossi, C. (2009). The optical characterization of chromophoric dissolved organic matter using wavelength distribution of absorption spectral slopes. *Limnol. Oceanogr.*, *54*(2), 590-597. https://doi.org/10.4319/lo.2009.54.2.0590

Lueker, T. J., Dickson, A. G., & Keeling, C. D. (2000). Ocean pCO2 calculated from dissolved inorganic carbon, alkalinity, and equations for K1 and K2: validation based on laboratory measurements of CO2 in gas and seawater at equilibrium. *Mar. Chem.*, *70*(1), 105-119. https://doi.org/https://doi.org/10.1016/S0304-4203(00)00022-0

Mari, X. (1999). Carbon content and C:N ratio of transparent exopolymeric particles (TEP) produced by bubbling exudates of diatoms. *Mar. Ecol. Prog. Ser.*, *183*, 59-71. https://doi.org/10.3354/meps183059

Mari, X., & Burd, A. (1998). Seasonal size spectra of transparent exopolymeric particles (TEP) in a coastal sea and comparison with those predicted using coagulation theory. *Mar. Ecol. Prog. Ser.*, *163*, 63-76. https://doi.org/10.3354/meps163063

Mari, X., & Kiørboe, T. (1996). Abundance, size distribution and bacterial colonization of transparent exopolymeric particles (TEP) during spring in the Kattegat. *J. Plankton Res.*, *18*(6), 969-986. https://doi.org/10.1093/plankt/18.6.969

Marie, D., Partensky, F., Jacquet, S., & Vaulot, D. (1997). Enumeration and Cell Cycle Analysis of Natural Populations of Marine Picoplankton by Flow Cytometry Using the Nucleic Acid Stain SYBR Green I. *Appl. Environ. Microbiol.* , *63*(1), 186-193. https://doi.org/https://doi.org/10.1128/aem.63.1.186-193.1997

Michels, J., Stippkugel, A., Lenz, M., Wirtz, K., & Engel, A. (2018). Rapid aggregation of biofilm-covered microplastics with marine biogenic particles. *Proc. Royal Soc. B.* https://doi.org/http://dx.doi.org/10.1098/rspb.2018.1203

Mintrop, L., Pérez, F. F., González-Dávila, M., Santana-Casiano, J. M., & Körtzinger, A. (2000). Alkalinity determination by potentiometry: intercalibration using three different methods. *Cienc. Mar.*, *26*(1), 23-27. https://doi.org/http://dx.doi.org/10.7773/cm.v26i1.573

Mustaffa, N. I. H., Ribas-Ribas, M., Banko-Kubis, H. M., & Wurl, O. (2020). Global reduction of in situ CO2 transfer velocity by natural surfactants in the sea-surface microlayer. *Proc. Math. Phys. Eng. Sci.*, *476*(2234), 20190763. https://doi.org/10.1098/rspa.2019.0763

Orr, J. C., Epitalon, J. M., & Gattuso, J. P. (2015). Comparison of ten packages that compute ocean carbonate chemistry. *Biogeosciences*, *12*(5), 1483-1510. https://doi.org/10.5194/bg-12-1483-2015

Ortega-Retuerta, E., Mazuecos, I. P., Reche, I., Gasol, J. M., Álvarez-Salgado, X. A., Álvarez, M., Montero, M. F., & Arístegui, J. (2019). Transparent exopolymer particle (TEP) distribution and in situ prokaryotic generation across the deep Mediterranean Sea and nearby North East Atlantic Ocean. *Prog. Oceanogr.*, *173*, 180-191. https://doi.org/https://doi.org/10.1016/j.pocean.2019.03.002

Pabortsava, K., & Lampitt, R. S. (2020). High concentrations of plastic hidden beneath the surface of the Atlantic Ocean. *Nat. Comm.*, *11*(1), 4073. https://doi.org/10.1038/s41467-020-17932-9

Paerl, H. W. (1975). Microbial attachment to particles in marine and freshwater ecosystems. *Microb. Ecol.*, *2*(1), 73-83. https://doi.org/10.1007/bf02010382

Pierrot, D., Lewis, E., & Wallace, D. W. R. (2006). MS Excel Program Developed for CO2 System Calculations. ORNL/CDIAC-105a. Carbon Dioxide Information Analysis Center, Oak Ridge National Laboratory, U.S. Department of Energy, Oak Ridge, Tennessee. doi: 10.3334/CDIAC/otg.CO2SYS_XLS_CDIAC105a

Pitta, P., Nejstgaard, J. C., Tsagaraki, T. M., Zervoudaki, S., Egge, J. K., Frangoulis, C., Lagaria, A., Magiopoulos, I., Psarra, S., Sandaa, R.-A., Skjoldal, E. F., Tanaka, T., Thyrhaug, R., & Thingstad, T. F. (2016). Confirming the "Rapid phosphorus transfer from microorganisms to mesozooplankton

in the Eastern Mediterranean Sea" scenario through a mesocosm experiment. *J. Plankton Res.*, *38*(3), 502-521. https://doi.org/10.1093/plankt/fbw010

Rahav, E., Shun-Yan, C., Cui, G., Liu, H., Tsagaraki, T. M., Giannakourou, A., Tsiola, A., Psarra, S., Lagaria, A., Mulholland, M. R., Stathopoulou, E., Paraskevi, P., Herut, B., & Berman-Frank, I. (2016). Evaluating the Impact of Atmospheric Depositions on Springtime Dinitrogen Fixation in the Cretan Sea (Eastern Mediterranean)—A Mesocosm Approach. *Front. Mar. Sci., 3*. https://doi.org/10.3389/fmars.2016.00180

Rahlff, J., Stolle, C., Giebel, H.-A., Brinkhoff, T., Ribas-Ribas, M., Hodapp, D., & Wurl, O. (2017). High wind speeds prevent formation of a distinct bacterioneuston community in the sea-surface microlayer. *FEMS Microbiol. Ecol., 93*(5), fix041-fix041. https://doi.org/10.1093/femsec/fix041

Rahlff, J., Stolle, C., Giebel, H.-A., Ribas-Ribas, M., Damgaard, L. R., & Wurl, O. (2019). Oxygen Profiles Across the Sea-Surface Microlayer—Effects of Diffusion and Biological Activity [Original Research]. *Front. Mar. Sci., 6*(11). https://doi.org/10.3389/fmars.2019.00011

Royer, S.-J., Ferrón, S., Wilson, S. T., & Karl, D. M. (2018). Production of methane and ethylene from plastic in the environment. *PLOS ONE, 13*(8), e0200574. https://doi.org/10.1371/journal.pone.0200574

Santschi, P. H., Chin, W.-C., Quigg, A., Xu, C., Kamalanathan, M., Lin, P., & Shiu, R.-F. (2021). Marine Gel Interactions with Hydrophilic and Hydrophobic Pollutants. *Gels, 7*(3), 83. https://www.mdpi.com/2310-2861/7/3/83

Savoca, M. S., Wohlfeil, M. E., Ebeler, S. E., & Nevitt, G. A. (2016). Marine plastic debris emits a keystone infochemical for olfactory foraging seabirds. *Science Advances, 2*(11), e1600395. https://doi.org/doi:10.1126/sciadv.1600395

Shen, M., Ye, S., Zeng, G., Zhang, Y., Xing, L., Tang, W., Wen, X., & Liu, S. (2020). Can microplastics pose a threat to ocean carbon sequestration? *Mar. Pollut. Bull., 150*, 110712. https://doi.org/https://doi.org/10.1016/j.marpolbul.2019.110712

Shiu, R.-F., Vazquez, C. I., Chiang, C.-Y., Chiu, M.-H., Chen, C.-S., Ni, C.-W., Gong, G.-C., Quigg, A., Santschi, P. H., & Chin, W.-C. (2020). Nano- and microplastics trigger secretion of protein-rich extracellular polymeric substances from phytoplankton. *Sci.Total. Environ., 748*, 141469. https://doi.org/https://doi.org/10.1016/j.scitotenv.2020.141469

Su, X., Yang, L., Yang, K., Tang, Y., Wen, T., Wang, Y., Rillig, M. C., Rohe, L., Pan, J., Li, H., & Zhu, Y.-g. (2022). Estuarine plastisphere as an overlooked source of N2O production. *Nature Communications, 13*(1), 3884. https://doi.org/10.1038/s41467-022-31584-x

Thompson, J. B. (2000). Microbial Whitings. In R. E. Riding & S. M. Awramik (Eds.), *Microbial Sediments* (pp. 250-260). Springer Berlin Heidelberg. https://doi.org/10.1007/978-3-662-04036-2_27

Thompson, J. B., Schultze-Lam, S., Beveridge, T. J., & Des Marais, D. J. (1997). Whiting events: biogenic origin due to the photosynthetic activity of cyanobacterial picoplankton. *Limnol. Oceanogr., 42*(1), 133-141. https://doi.org/10.4319/lo.1997.42.1.0133

Thornton, D. C. O. (2018). Coomassie Stainable Particles (CSP): Protein Containing Exopolymer Particles in the Ocean. *Front. Mar. Sci., 5*(206). https://doi.org/10.3389/fmars.2018.00206

Thornton, D. C. O., Brooks, S. D., & Chen, J. (2016). Protein and Carbohydrate Exopolymer Particles in the Sea Surface Microlayer (SML). *Front. Mar. Sci., 3*(135). https://doi.org/10.3389/fmars.2016.00135

Tsiola, A., Pitta, P., Callol, A. J., Kagiorgi, M., Kalantzi, I., Mylona, K., Santi, I., Toncelli, C., Pergantis, S., & Tsapakis, M. (2017). The impact of silver nanoparticles on marine plankton dynamics:

Dependence on coating, size and concentration. *Sci.Total. Environ.*, *601-602*, 1838-1848. https://doi.org/https://doi.org/10.1016/j.scitotenv.2017.06.042

Tsiola, A., Tsagaraki, T. M., Giannakourou, A., Nikolioudakis, N., Yücel, N., Herut, B., & Pitta, P. (2017). Bacterial Growth and Mortality after Deposition of Saharan Dust and Mixed Aerosols in the Eastern Mediterranean Sea: A Mesocosm Experiment. *Frontiers in Marine Science*, *3*. https://doi.org/10.3389/fmars.2016.00281

Upstill-Goddard, R. C. (2006). Air–sea gas exchange in the coastal zone. *Estuarine, Coastal and Shelf Science*, *70*(3), 388-404. https://doi.org/https://doi.org/10.1016/j.ecss.2006.05.043

Verdugo, P. (2012). Marine Microgels. *Annual Review of Marine Science*, *4*(1), 375-400. https://doi.org/doi:10.1146/annurev-marine-120709-142759

Wurl, O., Ekau, W., Landing, W. M., & Zappa, C. J. (2017). Sea surface microlayer in a changing ocean – A perspective. *Elementa-Sci. Anthrop.*, *5*(31). https://doi.org/http://doi.org/10.1525/elementa.228

Wurl, O., & Holmes, M. (2008). The gelatinous nature of the sea-surface microlayer. *Mar. Chem.*, *110*(1-2), 89-97. https://doi.org/10.1016/j.marchem.2008.02.009

Wurl, O., Stolle, C., Van Thuoc, C., The Thu, P., & Mari, X. (2016). Biofilm-like properties of the sea surface and predicted effects on air–sea CO2 exchange. *Prog. Oceanogr.*, *144*, 15-24. https://doi.org/https://doi.org/10.1016/j.pocean.2016.03.002

Yue, W.-z., Sun, C.-c., Shi, P., Engel, A., Wang, Y.-s., & He, W.-H. (2018). Effect of temperature on the accumulation of marine biogenic gels in the surface microlayer near the outlet of nuclear power plants and adjacent areas in the Daya Bay, China. *PLOS ONE*, *13*(6), e0198735. https://doi.org/10.1371/journal.pone.0198735

Zäncker, B., Bracher, A., Röttgers, R., & Engel, A. (2017). Variations of the Organic Matter Composition in the Sea Surface Microlayer: A Comparison between Open Ocean, Coastal, and Upwelling Sites Off the Peruvian Coast. *Front. Microbiol.* , *8*(2369). https://doi.org/10.3389/fmicb.2017.02369

Zäncker, B., Cunliffe, M., & Engel, A. (2018). Bacterial Community Composition in the Sea Surface Microlayer Off the Peruvian Coast. *Front. Microbiol.* , *9*(2699). https://doi.org/10.3389/fmicb.2018.02699

Zettler, E. R., Mincer, T. J., & Amaral-Zettler, L. A. (2013). Life in the "Plastisphere": Microbial Communities on Plastic Marine Debris. *Environ. Sci. Technol.*, *47*(13), 7137-7146. https://doi.org/10.1021/es401288x

Zhao, S., Zettler, E. R., Amaral-Zettler, L. A., & Mincer, T. J. (2021). Microbial carrying capacity and carbon biomass of plastic marine debris. *ISME J.*, *15*(1), 67-77. https://doi.org/10.1038/s41396-020-00756-2

Tables and Figures

Parameter / unit	ANOVA F	P value	Test	Mean Control	Mean MP	SE of difference	% of difference MP-C
TA (ULW) [µmol Kg^{-1}]	F (11, 43) = 3.138	**0.0035**	REML	2625.0	2631.0	1.77	0.2
DIC (ULW)* [µmol Kg^{-1}]	*F (11, 43) = 9.482*	***<0.0001***	*REML (time)*	2283.0	2286.0	0.94	0.1
pCO_2 (ULW) [µatm]	F (11, 43) = 4.279	**0.0003**	REML	420.20	409.10	3.78	-2.6
pH (ULW)	F (11, 43) = 4.552	**0.0001**	REML	8.064	8.075	0.00	0.14
CO_3^{2-} [µmol Kg^{-1}]	F (11, 43) = 2.814	**0.0075**	REML	243.10	246.20	1.09	1.3
CO_2 [µmol Kg^{-1}]	F (11, 43) = 3.845	**0.0007**	REML	13.09	12.78	0.11	-2.4
HCO_3^-* [µmol Kg^{-1}]	*F (11, 43) = 2.991*	***0.0049***	*REML (time)*	2027.0	2027.0	1.27	0.0
TEP (SML)* [10^6 mm^2 L^{-1}]	*F (6, 24) = 3.573*	**0.0113**	*RM ANOVA (time)*	493.50	641.70	60.30	30.0
TEP (SML) [10^6 particles L^{-1}]	F (6, 24) = 2.836	**0.0312**	RM ANOVA	61.06	77.44	5.53	26.8
TEP-C (SML)* [µg Carbon L^{-1}]	*F (6, 24) = 3.868*	***0.0077***	*RM ANOVA (time)*	324.30	424.80	49.43	31.0
CSP (SML) [10^6 mm^2 L^{-1}]	F (6, 24) = 4.932	**0.002**	RM ANOVA	682.30	854.50	55.72	25.2
CSP (SML) [10^6 particles L^{-1}]	F (6, 24) = 4.870	**0.0022**	RM ANOVA	75.93	113.57	8.24	49.6
Syn (SML) [10^6 cells L^{-1}]	F (5, 20) = 4.417	**0.0071**	RM ANOVA	64.28	65.15	3.01	1.4
HDNA-Syn (SML)* [10^6 cells L^{-1}]	*F (5, 20) = 21.54*	***<0.0001***	*RM ANOVA (time)*	1.46	1.81	0.22	23.5
LDNA-Syn (SML) [10^6 cells L^{-1}]	F (5, 20) = 4.947	**0.0041**	RM ANOVA	62.85	63.35	2.84	0.8
$S_{275-295}$ (SML) [nm^{-1}]	F (6, 24) = 3.146	**0.0203**	RM ANOVA	0.01	0.01	0.00	4.1
a(355) nm (SML) [m^{-1}]	F (6, 24) = 1.090	0.3963	RM ANOVA	3.89	3.90	0.05	0.1
DOC (SML) [mg L^{-1}]	F (1, 4) = 0.02581	0.6927	REML	1.23	1.21	0.11	-1.5
H. Bacteria (SML)* [10^8 cells L^{-1}]	*F (6, 21) = 9.815*	***<0.0001***	*REML (time)*	4.46	4.31	0.42	-3.4
HDNA H. Bacteria (SML)* [10^8 cells L^{-1}]	*F (6, 21) = 10.40*	***<0.0001***	*REML (time)*	3.13	2.98	0.39	-4.8
LDNA H. Bacteria (SML)* [10^8 cells L^{-1}]	*F (6, 21) = 13.07*	***<0.0001***	*REML (time)*	1.27	1.34	0.05	5.3

Table 1 Repeated Measures Two-Way ANOVA or Mixed effects Model (REML) Analysis Table where the fixed factor is the "treatment" (MP/ no MP) and the random effect is the time. Results are shown as the interaction of "treatment x time" unless otherwise noted. Replicates within the treatments have been

assumed having equal variability of differences. (*) indicates differences that have been observed between MP and Control in time. Significant differences are accepted for p< 0.05.

$S_{275-295}$ [nm^{-1}], SML	pCO_2 [µatm], ULW	DOC [mg L^{-1}], SML	Heterotrophic bacteria [cells L^{-1}], SML	CSP [mm^2 L^{-1}], SML	*Synechococcus* [cells L^{-1}], SML
Spearman r	0.51	0.45	0.34	0.35	-0.61
p	< 0.001	0.004	0.032	0.024	< 0.0001
n	42	39	39	42	39

Table 2 Spearman r correlation table reporting significant correlations of Spectral Slope in the SML between 275 and 295 nm ($S_{275-295}$) to pCO_2 (ulw), and DOC, Heterotrophic Bacteria, CSP and Synechocccus cells in the SML.

***Synechococcus* [cells L^{-1}]**	***TA* [µmol Kg^{-1}]**	***DIC* [µmol Kg^{-1}]**	***pH in***	***pCO_2 [µatm]***	***CO_3^{2-} [µmol Kg^{-1}]***	***CO_2 [µmol Kg^{-1}]***
Spearman r	0.531	0.429	0.344	-0.33	0.336	-0.321
p	0.000557	0.00664	0.0323	0.0406	0.0368	0.0465
n	39	39	39	39	39	39

TEP-C [µg C L^{-1}]	***TA* [µmol Kg^{-1}]**	***DIC* [µmol Kg^{-1}]**	***pH in***	***pCO_2 [µatm]***	***CO_3^{2-} [µmol Kg^{-1}]***	***CO_2 [µmol Kg^{-1}]***
Spearman r	0.511	0.273	0.434	-0.433	0.481	-0.437
p	0.000592	0.0798	0.00428	0.00438	0.00137	0.00395
n	42	42	42	42	42	42

Table 3 Spearman r correlation table between Synechococcus and TEP-Carbon (TEP-C) in the SML to Total Alkalinity (TA), DIC, pH, pCO_2 CO_3^{2-} and CO_2 in the bulk water of the mesocosms.

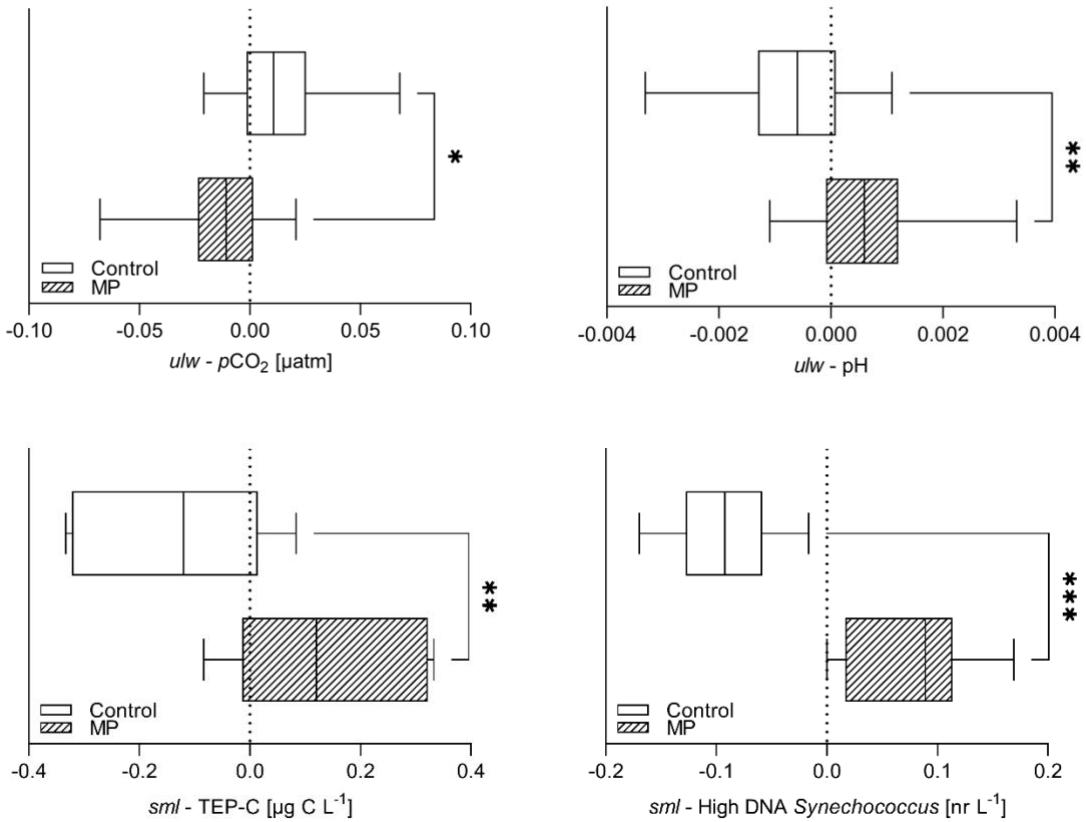

Figure 1 Boxplots represent normalized anomalies and 5-95 percentiles for underlying water (ulw) pCO_2, pH, and for sea-surface microlayer (SML) TEP-carbon (TEP-C) and High DNA containing Synechococcus cells. Stars indicate the level of significance in the differences between control and MP mesocosms based on Mann-Whitney tests on normalized anomalies (pCO2, pH, and unpaired t-tests (TEP-C and High DNA Synechococcus cells).

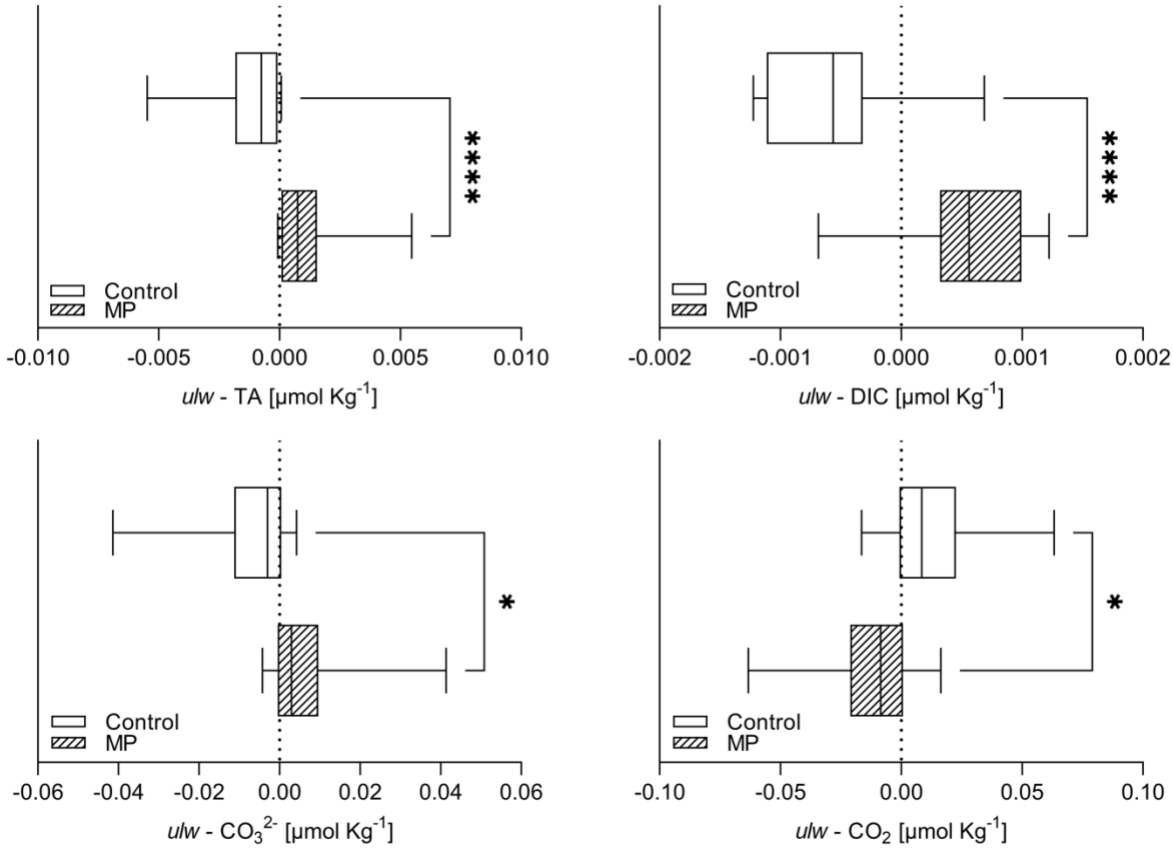

769
770 *Figure 2 Boxplots that represent normalized anomalies and 5-95 percentiles for underlying water (ulw)*
771 *Total Alkalinity (TA), Dissolved Inorganic Carbon (DIC), CO_3^{2-} and CO_2. Stars indicate the level of*
772 *significance in the differences between control and MP mesocosms based on Mann-Whitney test (TA,*
773 *CO_3^{2-} and CO_2) and unpaired t-test (DIC).*

774

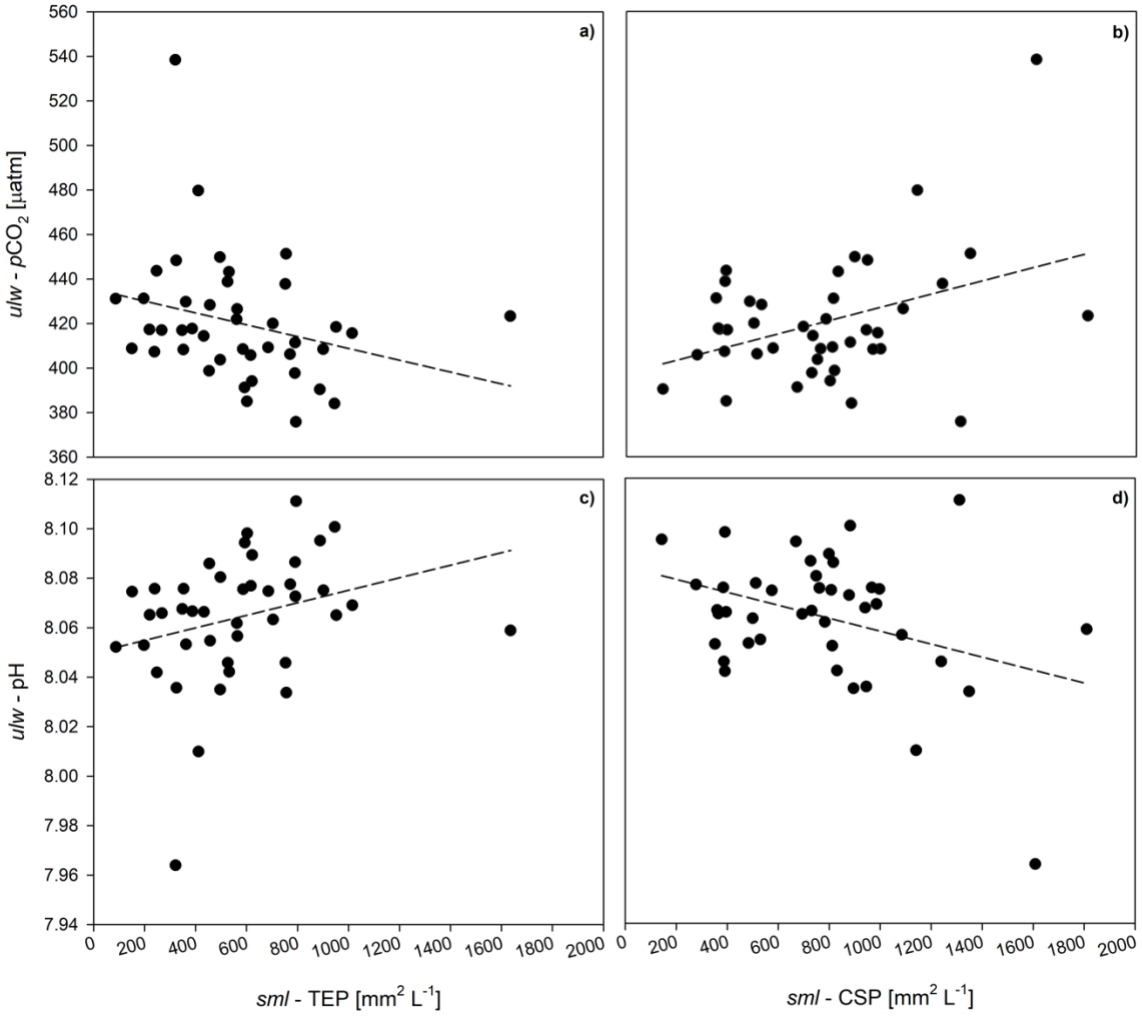

Figure 3 Panels a, b: Multiple linear regression between pCO_2 in the underlying water (ulw) and the presence of marine gels (TEP, a; CSP, b) in the sea-surface microlayer (SML).

Panels c, d: Multiple linear regression between pH in the underlying water (ulw) on marine gels (TEP, c; CSP, d) in the sea-surface microlayer (SML) according to the equation:

$$pH = 8.070 + 0.0000471\ TEP\ [mm^2\ L^{-1}] - 0.0000421\ CSP\ [mm^2\ L^{-1}].$$

For the regression, $R^2 = 0.365$, $p < 0.001$, $F = 11.22$, $DF = 2$. All panels have been displayed separately to better visualize the trends.

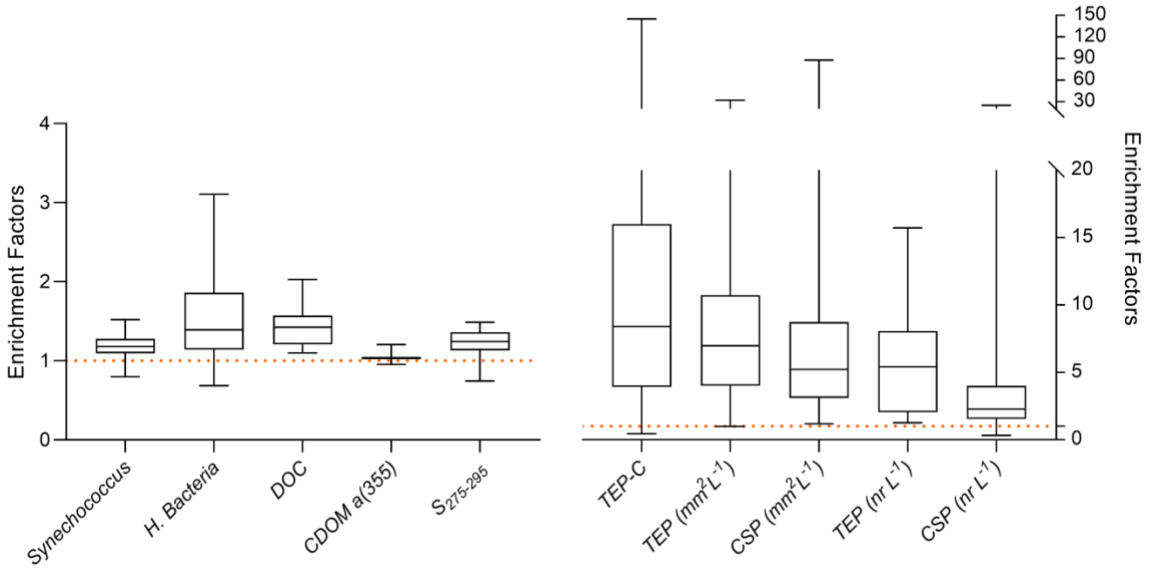

784

785 *Figure 4 Enrichment factors for SML parameters compared to underlying water considering both*
786 *treatments. The dashed orange line is set on both graphs to EF = 1 which means no real differences*
787 *between SML concentration and underlying water concentration.*

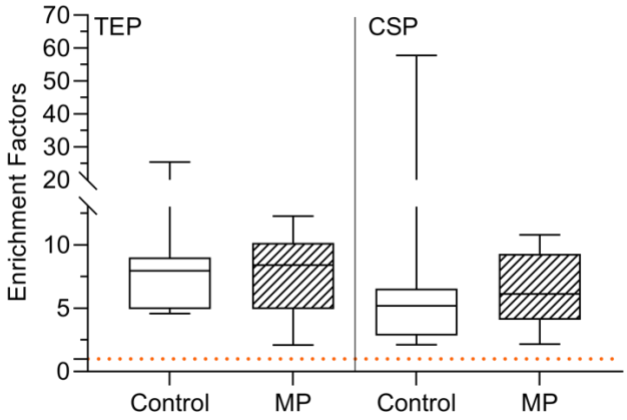

788

789 *Figure 5 Enrichment Factors for the concentration of marine gels TEP and CSP, expressed as area mm²*
790 *L⁻¹, between Control and MP mesocosms. The orange dashed line indicates EF = 1. Repeated Measures*
791 *two-way ANOVA tests (Table S4) have evidenced significant differences between EFs.*

792

793